PNNL-39360

Fabrication of ceramic to metal graded structure for high temperature CSP receiver application using solid state additive manufacturing

May 2026

1 Saumyadeep Jana
2 Jon L Helgeland
3 Josef Matyas
4 Devesh Chouhan

Prepared for the U.S. Department of Energy
under Contract DE-AC05-76RL01830

PACIFIC NORTHWEST NATIONAL LABORATORY
operated by
BATTELLE
for the
UNITED STATES DEPARTMENT OF ENERGY
under Contract DE-AC05-76RL01830

Printed in the United States of America

Available to DOE and DOE contractors from
the Office of Scientific and Technical Information,
P.O. Box 62, Oak Ridge, TN 37831-0062
www.osti.gov
ph: (865) 576-8401
fox: (865) 576-5728
email: reports@osti.gov

Available to the public from the National Technical Information Service
5301 Shawnee Rd., Alexandria, VA 22312
ph: (800) 553-NTIS (6847)
or (703) 605-6000
email: info@ntis.gov
Online ordering: http://www.ntis.gov

PNNL-39360

Fabrication of ceramic to metal graded structure for high temperature CSP receiver application using solid state additive manufacturing

May 2026

1 Saumyadeep Jana
2 Jon L Helgeland
3 Josef Matyas
4 Devesh Chouhan

Prepared for
the U.S. Department of Energy
under Contract DE-AC05-76RL01830

Pacific Northwest National Laboratory
Richland, Washington 99354

Summary

The overarching goal of this project is to come up with an innovative joining solution for integration of SiC ceramic to structural materials such as stainless steels (SS)/Ni-base alloys, where intimate metallurgical bonding between SiC ceramic and the structural metallic alloy is demonstrated at the interface. Implementation of a simple, yet robust joining method would help in increasing the application space of SiC in a high-temperature CSP (concentrated solar power) plant, especially in the receiver section. This research goal has been achieved by creating a functionally graded material (FGM) interface between SiC and the selected structural material with the help of powder metallurgy (PM) approach and demonstrate intimate metallurgical bonding between monolithic RB-SiC and 316L stainless steel alloy blanks.

As a first step, suitable interlayer alloys that can form metallurgical bonding between SiC and selected metallic alloys have been selected. Appropriate heat treatment cycle was developed to achieve good bonding between SiC/interlayer alloy/metal couple. Subsequently, SiC/interlayer alloy/metallic alloy bulk coupons (20 x 20 x 10 mm) were fabricated by PM-based additive manufacturing (AM) method to achieve compositional grading of selected interlayer alloys. **Specifically, PM-based tape casting process, which is suitable for manufacturing thin films, has been used to create a multi-stack structure and densified through high temperature sintering to demonstrate metallurgical bonding between SiC and selected structural alloy.** Successful implementation of fabricating FGM interlayer through PM-based method provides a unique joining solution of SiC to metals, since there is large mismatch in the coefficient of thermal expansion (CTE), elastic modulus and strength and ductility values between SiC and structural alloys such as 316L SS, Ni-base alloys. Having a compositionally graded interface between SiC and metal will help in gradual change in CTE/modulus values between SiC and the selected metal *to better* manage residual stress at interface. Major objectives of this project are the following:

1. **Selection of appropriate interlayer alloy to create the FGM interface.**
2. **Use of tape casting process to create the desired interlayer inserts.**
3. **Development of sintering method to create metallurgical bonding between SiC and selected metal using appropriate FGM insert.**
4. **Demonstrate success of the joining method through mechanical tests and microscopy**.

Technical Achievements

An extensive literature review of available joining solutions for ceramics have been carried out. Special focus has been placed on ceramic to metal joining. Available information on joining of non-oxide ceramic such as SiC to metal is very limited. A detailed table has been created to capture how joining has been caried out between SiC to SiC, and SiC to metal using various joining methods such as brazing, diffusion bonding etc. Also, a list of materials that could be placed as interlayer between SiC to SiC or metal has been prepared. **Based on the prepared list, we have obtained selected powders that has been used in creating the interlayer through tape casting method. List of selected powders are the following: Si, C, Ti, Cr, Ni, Mo, and W.** Monolithic SiC substrates have been obtained in two forms, (i) sintered SiC (S-SiC), and (ii) reaction-bonded SiC (RB-SiC). For metal substrate, following alloys have been identified: (i) 316L SS, (ii) Kanthal APMT, (iii) Inconel 625, and (iv) Haynes 282. **Joining effort study has mostly focused on creating metallurgical bonding between RB-SiC and 316L SS alloy.**

Tape casting trial has been carried out with various configurations; (i) single layer with composite compositions, and (ii) multilayers with various target compositions. A final stack with thickness ~1 mm or higher has been fabricated by consolidating multiple individual tapes together. Tape casting process optimization has been aimed at (i) increasing solid volume fraction loading, and (ii) creating a compositionally graded stack. Tape casting slurry chemistry has been refined to minimize porosity in tapes after sintering. This has been demonstrated by documenting TGA weight loss of 12–15% in initial tapes to 1% with recent optimizations. Small-scale heat treatment of tape cast stacks have been carried out at target temperature and environment using DSC (differential scanning calorimetry) technique. Initial evidence of solid-state reaction in tape cast stacks has been noted through microscopy.

Following the successful completion of small-scale heat treatment experiments, bulk joining trials were conducted between monolithic silicon carbide (SiC) substrates and structural alloy 316L stainless steel coupons. These trials utilized a furnace heat treatment approach, where various target compositions—prepared through the tape casting method—were placed as interlayers between SiC blanks and 316L stainless steel blanks. The heat treatment process was carefully optimized in terms of temperature and environment to enhance the quality of the metallurgical bond at the interface. These efforts focused on achieving a robust and intimate metallurgical connection between the SiC ceramic and the stainless steel, aligning with the project's overarching objective of developing a reliable joining solution for high-temperature applications.

A thorough evaluation of the bulk silicon carbide substrate, tape-cast interlayer, and 316L stainless steel bulk blank was performed utilizing optical microscopy (OM), scanning electron microscopy (SEM), and energy-dispersive X-ray spectroscopy (EDS) analysis. Additionally, preliminary mechanical performance metrics for the interface were acquired via microhardness testing.

This project was conducted under the Small Innovative Projects in Solar (SIPS) program, which is designed to pursue high-risk, high-reward research initiatives. The findings have shown that silicon carbide can be effectively joined to structural metals such as stainless steel by utilizing an optimized tape casting methodology. Through careful enhancement of the tape casting process and the deliberate selection of interlayer chemistry and design, robust metallurgical bonds between SiC and 316L SS can be achieved.

The research directly aligns SIPS objectives by addressing a significant technical challenge—joining ceramics like silicon carbide to metals for high-temperature applications. The project's innovative approach, which included developing a graded interlayer using tape casting and optimizing both composition and process parameters, embodies the SIPS spirit of pursuing transformative solutions that carry both high risk and high potential impact. The successful demonstration of metallurgical bonding between silicon carbide and stainless steel not only validates the project's hypothesis but also delivers a new joining strategy that could unlock advancements in solar thermal technology and industrial decarbonization. In this way, the research goal has fully realized the intended SIPS outcome: pioneering a novel, practical solution to a complex materials integration problem, with broad relevance for the solar and energy sectors.

Impact:

Silicon carbide is a critical material in advanced engineering, valued for its hardness, thermal stability, and resistance to corrosion. These properties make it ideal for high-temperature environments such as solar energy systems and industrial applications. This project tackled the challenge of bonding ceramics to metals, particularly non-oxide ceramics like SiC, by implementing an advanced joining technique.

Optimizing tape casting and furnace heat treatment presents an effective methodology for joining SiC to metals, contributing to the advancement of manufacturing processes that support industrial decarbonization and clean energy initiatives. This technique aligns with the objectives of the Solar Energy Technologies Office by facilitating the development of SiC-based volumetric receivers capable of delivering air at temperatures exceeding 1000°C.

By addressing the challenges associated with metal-SiC bonding, this research enhances solar-driven industrial heating and provides a foundation for emerging technologies in solar thermal systems. These advancements further Department of Energy priorities, including fusion energy, concentrating solar power, and advanced heat exchangers, thereby promoting the transition to clean energy and supporting the growth of sustainable industry.

Introduction

In CSP plants, the central receiver reaches the highest temperatures due to concentrated solar radiation. There are multiple receiver designs for different heat-transfer media and temperature ranges. Tubular external receivers, common in molten-salt and steam towers, use exposed tubes and typically operate at 600–650 °C. Volumetric receivers [1], feature porous ceramics for internal absorption, enabling air outlet temperatures of 850–1200 °C suitable for advanced cycles. Achieving temperatures above 750 °C in the receiver section is key for higher CSP plant efficiency.

Volumetric receivers offer several technical advantages that make them a leading architecture for next generation concentrating solar power (CSP) systems. Their most significant merit is the volumetric absorption of solar radiation, where energy is absorbed throughout a porous three-dimensional ceramic structure rather than solely at the surface. This produces a favorable temperature inversion in which the irradiated surface remains relatively cool while the working fluid—typically pressurized air—reaches very high outlet temperatures. This effect enables substantially higher operating temperatures than tubular metallic receivers, which are limited by alloy softening and oxidation at elevated temperatures. In addition, the porous architecture enhances convective heat transfer due to large internal surface area, improving receiver efficiency and reducing thermal gradients that can drive mechanical failure. This uniform heat distribution improves reliability under high flux transients [2]. The combination of high temperature capability, superior heat transfer performance, and material robustness makes volumetric receivers a promising solution for advanced CSP systems targeting higher efficiency and lower levelized cost of heat and electricity.

Volumetric receivers for high temperature CSP systems require materials capable of withstanding extreme radiative flux, high operating temperatures (> 750 °C), steep thermal gradients, and oxidative environments. Silicon carbide (SiC) and silicon infiltrated SiC (Si SiC/RB-SiC) are the preferred absorber materials for volumetric receivers [3,4] because they uniquely combine high temperature capability, strong optical performance, and exceptional environmental durability. SiC based ceramics maintain structural integrity and thermal conductivity at temperatures approaching 1400 °C, enabling efficient heat absorption under extreme solar flux. Their high solar absorptance and thermal conductivity promote uniform volumetric heating while minimizing thermal gradients. SiC and Si SiC also exhibit excellent oxidation and thermal shock resistance, essential for repeated sun cycling. In addition, their porous foam or reticulated structures provide large internal surface area, enabling highly efficient air–solid heat transfer required for advanced CSP operation. Integration of porous SiC absorber structures into a structural metallic housing is essential because SiC, while thermally superior, is brittle and cannot provide the mechanical strength, pressure containment, or structural stability required in high temperature volumetric receivers. Metallic supports accommodate thermal stresses, enable mounting and sealing, and form the pressure boundary for air or sCO_2 flow. Suitable alloys include 316L stainless steel and Ni based superalloys.

Joining silicon carbide (SiC) to stainless steel is a major manufacturing challenge due to the fundamental incompatibility between ceramic and metal behavior. SiC cannot be fusion welded to steel because SiC sublimes rather than melts, and the melting points differ significantly, preventing any metallurgical fusion. Active metal brazing is possible [5] but limits the assembly to the softening temperature of the braze, restricting high temperature CSP operation. Large mismatch in the coefficient of thermal expansion (CTE) —SiC ($\sim 4\times10^{-6}$ K^{-1}) vs. steel ($\sim 15\times10^{-6}$ K^{-1})—makes joining effort even more challenging.

This study examines the viability of utilizing a purpose-engineered interlayer to achieve robust joining between a silicon carbide (SiC) ceramic substrate and a 316L stainless steel (SS) metallic substrate. The interlayer is strategically designed to promote metallurgical bonding at both the ceramic and metal interfaces when subjected to high-temperature thermal treatments. Fabrication of the interlayer is accomplished via a powder metallurgy route, which enables precise control over material composition and microstructure. The process is tailored to produce a compositional gradient across the interlayer thickness, thereby mitigating issues associated with thermal expansion coefficient and elastic modulus mismatches between SiC and 316L SS. This graded architecture is intended to enhance joint reliability and structural integrity under the severe thermal and mechanical stresses characteristic of advanced CSP receiver environments.

1.0 Interlayer material and substrate selection

A comprehensive literature review was conducted to assess the current advancements in SiC joining, as summarized in Table 1.0. Numerous techniques have been extensively investigated for joining SiC to SiC ceramics, with the results detailed in Table 1.0. In contrast, research on the joining of SiC to metals, such as stainless steel, remains relatively limited.

Several elemental materials have been chosen as joining solutions for silicon carbide to silicon carbide or silicon carbide to metals. **Some of these elements include silicon (Si), carbon (C), titanium (Ti), chromium (Cr), nickel (Ni), molybdenum (Mo), and tungsten (W).** In this study, the powdered forms of these elements were utilized for the fabrication of the interlayer.

Table 1.0 SiC joining literature review summary

Substrate 1	Interface alloy	Substrate 2	Method	Source
RB-SiC	Ag-Cu-Ti	316LSS	Brazing	Am. Cermic. Soc. Bull., 64 [2] 322-24 (1985)
S-SiC				
S-SiC	Mo	316LNSS	Diffusion bonding	https://doi.org/10.1080/14786435.2021.1988746
	Mo-Cu			
	Mo-Ni-Cu-Ni			
S-SiC	W-Pd-Ni	Fe-18Cr (ferritic steel)	Diffusion bonding	DOI:10.1111/j.1744-7402.2009.02461.x
RB-SiC (free Si = 13 wt.%)	Nb	304LSS	Diffusion bonding	JOURNAL OF MATERIALS SCIENCE LETTERS 10 (1991) 339-340
S-SiC				
SiC (Reaction bonded, Sintered)	Carbon paste + Si-alloy	SiC (Reaction bonded, Sintered)	Reaction forming	https://www.sciencedirect.com/science/article/pii/S1359646297002339
SiC (Reaction bonded, Sintered)	Ti + Si	SiC (Reaction bonded, Sintered)	Diffusion bonding	https://www.sciencedirect.com/science/article/pii/S1738573316000814
	Ti foil			https://link.springer.com/article/10.1007/BF00552387
SiC (Reaction bonded, Sintered)	Ti foil		Spark plasma sinter	https://www.sciencedirect.com/science/article/pii/S0955221913005967
SiC	Nb, Ti, W, Mo, Ta Mo shows best joint	SiC	Metal foil diffusion bonding	https://www.osti.gov/biblio/755392
				https://www.sciencedirect.com/science/article/pii/S0022311513011410
SiC	Al2O3-Y2O3-SiO2	SiC	Laser melting	https://www.sciencedirect.com/science/article/pii/S0029549304000871#BIB16
	various glass ceramics		hot press	https://www.sciencedirect.com/science/article/pii/S0022311510009827
	NITE			
SiC	Si + TiC	SiC	Hot press	https://www.sciencedirect.com/science/article/pii/S0022311507005582
SiC	Si-Cr alloy	SiC	Brazing	https://www.sciencedirect.com/science/article/pii/S0022311504002648
	Ni-Ti-Si			https://www.sciencedirect.com/science/article/pii/S0029549315006081?via%3Dihub

Sintered SiC (S-SiC) and reaction-bonded SiC (RB-SiC) substrates have been utilized as 50x50x20 mm blanks, in this study. Comprehensive phase analysis and microscopy were conducted, with XRD plots of SiC substrates presented in Fig. 1. The analysis reveals that hexagonal α-SiC constitutes the predominant phase in both S-SiC and RB-SiC. Additionally, free carbon was detected in S-SiC, whereas free silicon was observed in RB-

SiC. Representative SEM images for RB-SiC are illustrated in Fig. 2, exhibiting sizeable SiC particles within the matrix. These particles are encompassed by an extensive network of free silicon, as demonstrated by the EDS elemental map in Fig. 3. Furthermore, Fe-rich particles were occasionally identified in the RB-SiC matrix. The RB-SiC blanks display high density and minimal porosity. In comparison, SEM images and EDS elemental mapping for S-SiC blanks (Fig. 4) indicate SiC as the primary phase, accompanied by numerous TiN particles. S-SiC blanks exhibit lower density than RB-SiC, with significant porosity observed.

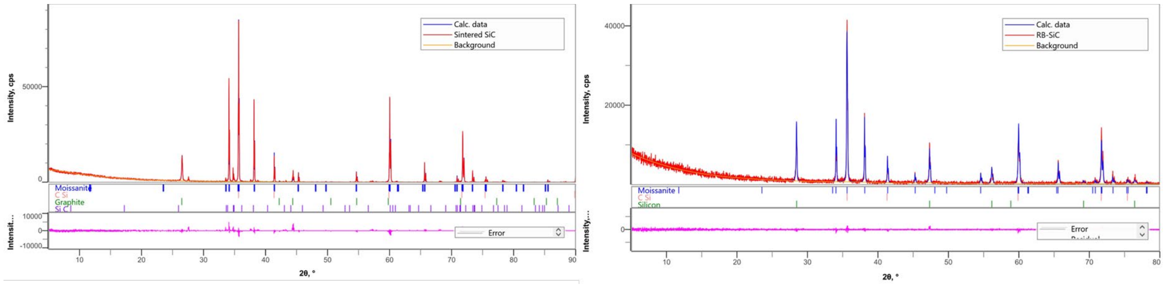

Fig. 1 XRD plot of (i) sintered SiC and (ii) reaction bonded SiC

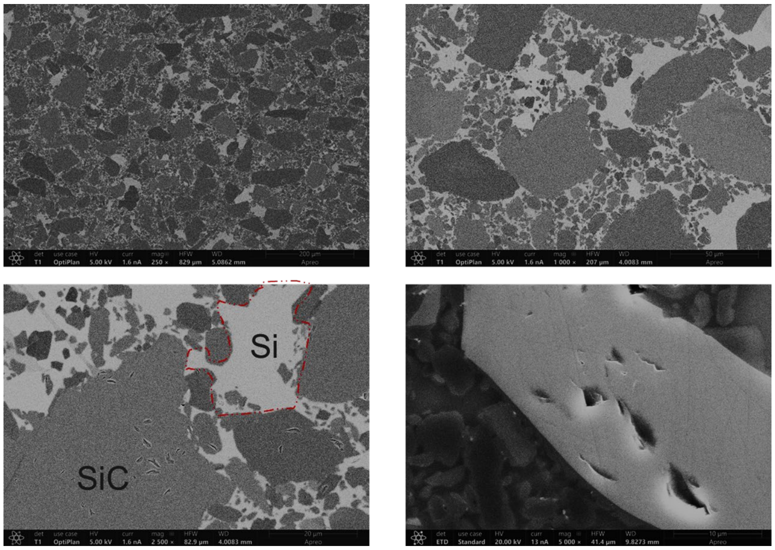

Fig. 2 SEM images obtained RB-SiC blank. SiC particles remain embedded in a continuous network of free Si.

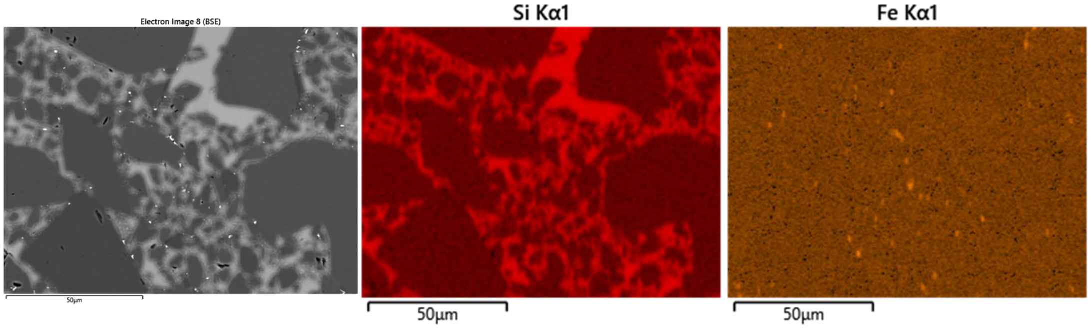

Fig. 3 EDS elemental map from RB-SiC confirms free Si, and occasional free Fe.

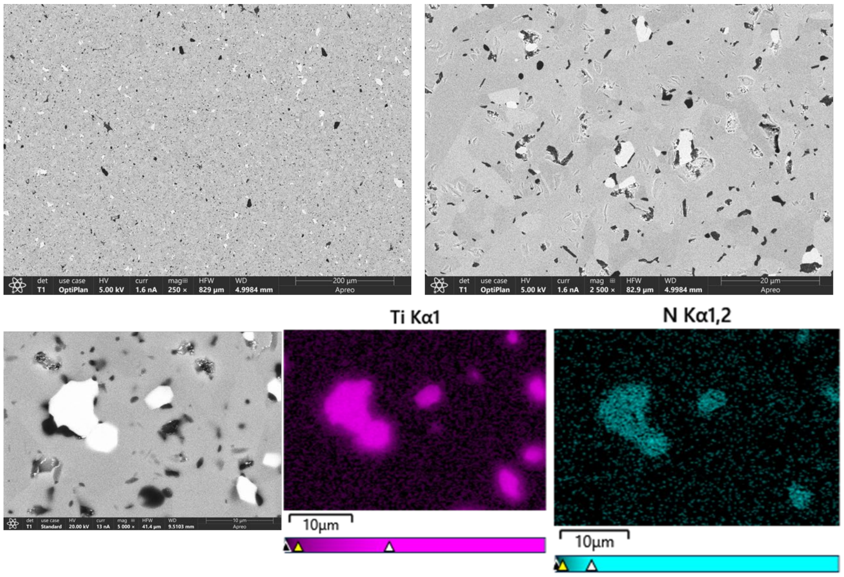

Fig. 4 SEM images and EDS elemental map obtained from S-SiC blanks. Numerous TiN particles are noted in S-SiC blanks. S-SiC is more porous than RB-SiC.

2.0 Fabrication of graded interface joint between SiC and metal substrate using tape casting

Tape casting process development

The tape casting method has been established for producing a compositionally graded interlayer insert between SiC and potential metal substrates. Initially, dispersants, binders, plasticizers, and solvents are combined with selected inorganic powders to formulate a target slurry, which is subsequently deposited as a thin layer onto a carrier film using a doctor blade technique. Careful selection of appropriate binders and optimization of inorganic powder size and morphology are essential to creating a high-quality slurry and achieving optimal green density. Tape casting enables the fabrication of multiple green films with tailored chemistries. These films are then stacked and laminated, followed by debinding and sintering processes. A schematic illustration of the tape casting procedure is provided in Fig. 5.

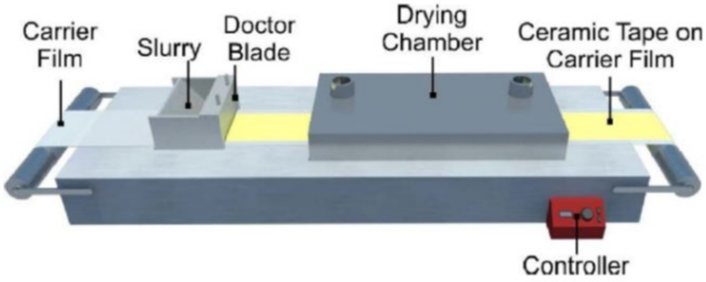

Fig. 5 Tape casting process schematic

To begin with, tape casting process has been carried out to create a 1 mm thick stack made of Si, C, Ti and Ni powder. A casting slurry was prepared by mixing mentioned inorganic powders with a blend of binders, plasticizers and solvents. For good mixing of the slurry, inorganic powders in desired quantity are set to mix with polymeric compounds in a roller mill for more than 24 hr. Subsequently, thin tapes are fabricated from this slurry by pouring on a moving mylar film. Thickness of the cast tape is adjusted by using an appropriate doctor blade. Initially cast tapes were ~150-300 µm in thickness. Multiple tape cast films were then put together, and laminated to create a thicker stack, which is ~ 1 mm in thickness. Fig. 6 shows the tape casting facility at PNNL, and an image of the tape cast and laminated film made of Si, C, Ti and Ni powder mixed with organic binders.

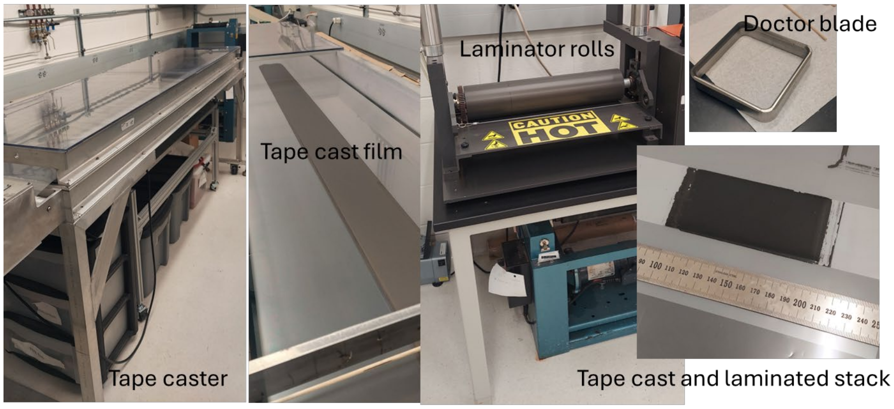

Fig. 6 Tape casting facility at PNNL

An image of the laminated tape cast Si-C-Ti-Ni stack in green state is shown in Fig. 7. Si, Ni and Ti powders are noted to be uniformly distributed in the laminated stack. There are a few large Si particles noted, which is due to relatively coarse grade of Si powders used in making the slurry. Ni powder appears to be very well mixed. Similar observation is made for Ti powder.

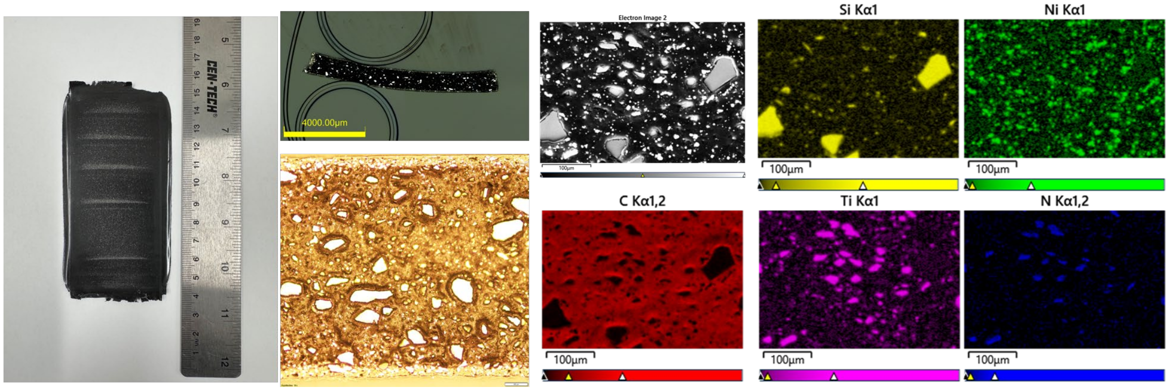

Fig. 7 Laminated stack (~1 mm thick) of multiple tape cast films made of Si-C-Ti-Ni mixture.

Subsequently, a multiple layer laminated stack has been fabricated using tape casting method. This stack is made Si-C/Ti/Ni combination. Fig. 8 shows a cross-section SEM image of the stack, made of Si-C; Ti and Ni tapes in green state. EDS analysis shows that the layers are maintaining distinct chemical composition, and are not getting intermixed during lamination process. Subsequently, this multi-chemistry stack has been heat treated to find the types of chemical reaction that can take place between individual elements.

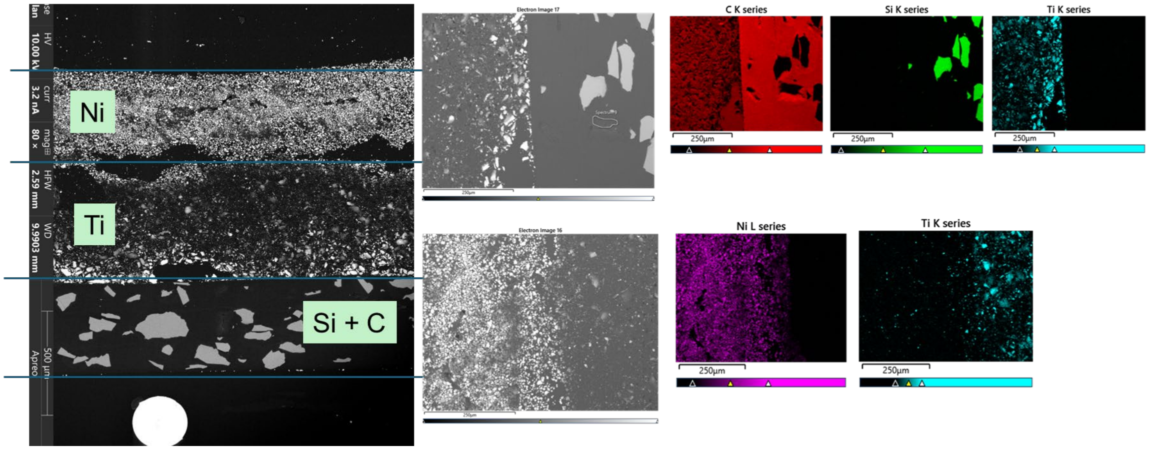

Fig. 8 Cross-section image of a multi-chemistry stack. 1st layer – Si + C; 2nd layer – Ti; 3rd layer – Ni; EDS confirms retention of chemistry after lamination. No intermixing noted after lamination.

One of our objectives in optimizing the tape casting process was to decrease the weight percentage of organics in the slurry. This reduction aimed to increase the solid volume fraction, thereby resulting in higher density after sintering. During initial trials, the organic content was relatively high at approximately 15 weight percent. We subsequently sought to lower this value and evaluate whether the slurry could still be effectively tape cast. There is always a possibility of encountering challenges in tape casting when the organic content is reduced, as these components are important for ensuring sufficient flexibility and flowability in the slurry. To address this, we progressively decreased the organic content, targeting levels of 3%, and ultimately less than 1% by weight. The outcomes were verified through TGA analysis, as presented in Figure 9. **Currently, we are making tape cast slurries with less than 1 wt% organics, and we can generate very good quality films.**

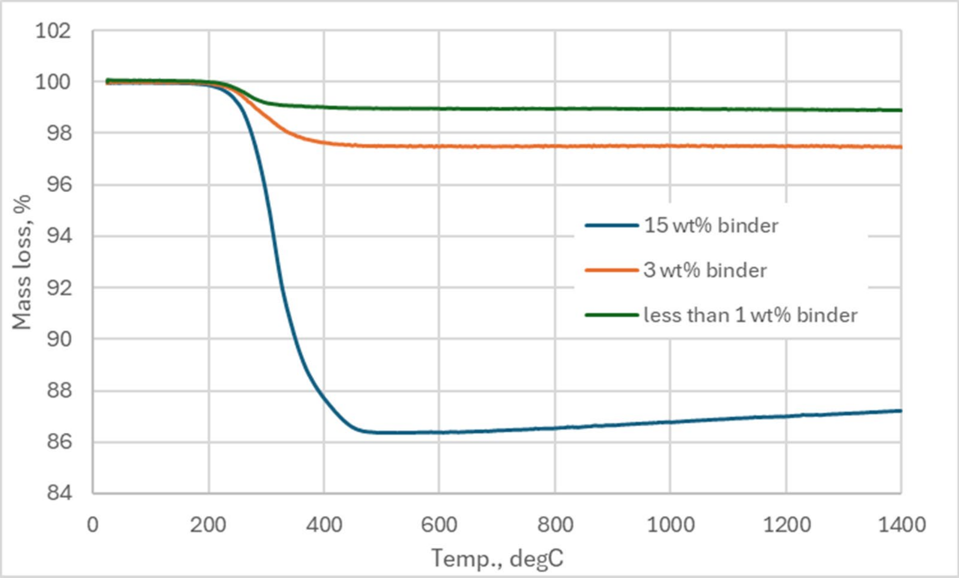

Fig. 9 TGA plots for tape cast slurry. Organics content optimization study confirms less than 1 wt.% slurry can be tape cast

Upon completion of our tape casting optimization study, we demonstrated that tape casting is achievable with an organic content below one weight percent. Thin tapes, approximately 200 microns in thickness, can be efficiently tape cast using our optimized process. Furthermore, tape casting enables the production of multi-chemistry stacks, allowing each chemistry to be preserved in the green state. This capability is crucial for developing functionally graded interlayers.

3.0 Heat treatment optimization at small scale to demonstrate reaction sintering

The sintering temperature of SiC is approximately 2000°C, whereas potential FGM alloy layer candidates can be processed at around 1300–1400°C. Addressing the disparity in sintering temperatures between SiC and candidate FGM alloys requires the development of a reactive sintering approach. One method to facilitate reactive sintering involves tape casting elemental silicon powder and carbon black in a stoichiometric ratio, followed by deposition of the FGM alloy layer and the target substrate metal layer. Elemental silicon and carbon black are subsequently converted into SiC via solid-state reaction, which has been demonstrated to occur at approximately 1300°C through volume chemical synthesis. This process enables effective bonding with both the FGM interlayer and the target metal layer during high-temperature sintering.

To pursue reaction sintering, initial heat treatment was performed on composite tape-cast and laminated Si-C-Ti-Ni stacks. The heat treatments were conducted at 1400°C in argon and at 1400°C in air using a differential scanning calorimetry (DSC) instrument. Small discs (5 mm diameter) were rapidly heated inside the DSC under the designated atmospheres to 1400°C, followed by cooling without an isothermal hold. Optical micrographs presented in Figure 10 illustrate the influence of heat treatment on the composite Si-C-Ti-Ni stack. Large, bright particles present in the green tape are identified as elemental silicon. It is evident that the number of large silicon particles is considerably lower after heat treatment in argon than in air. A key distinction between heat treatment in air and argon is that elemental carbon powder combusts when heated in air but remains under argon. The observed reduction in the size of elemental silicon particles during heat treatment in an argon atmosphere suggests the potential for reaction sintering.

To further elucidate the characteristics of reaction sintering, scanning electron microscopy (SEM) was employed on heat-treated composite Si-C-Ti-Ni stacks, as depicted in Figure 11. The specimen subjected to heating in air exhibits pronounced porosity, indicative of carbon powder burnout, which is corroborated by the thermogravimetric analysis (TGA) trace. In contrast, the sample processed under argon demonstrates greater density. A significant reduction in the size of silicon particles originally present in the green state tape is also observed. At higher magnification (Figure 12), the argon-treated sample displays a highly uniform and fine microstructure (<100 nm), which provides clear evidence of reaction sintering. This refined microstructure is absent in samples subjected to heat treatment in air. The microstructure of the Si-C-Ti-Ni composite following air treatment differs significantly. The EDS elemental map of the air-treated Si-C-Ti-Ni sample, shown in Fig. 13, indicates no substantial reaction between Si and either Ti or Ni. However, interaction between Ti and Ni is evident. The formation of various oxides, and possibly nitrides, was observed and further confirmed by XRD analysis, when the sample was heated in air.

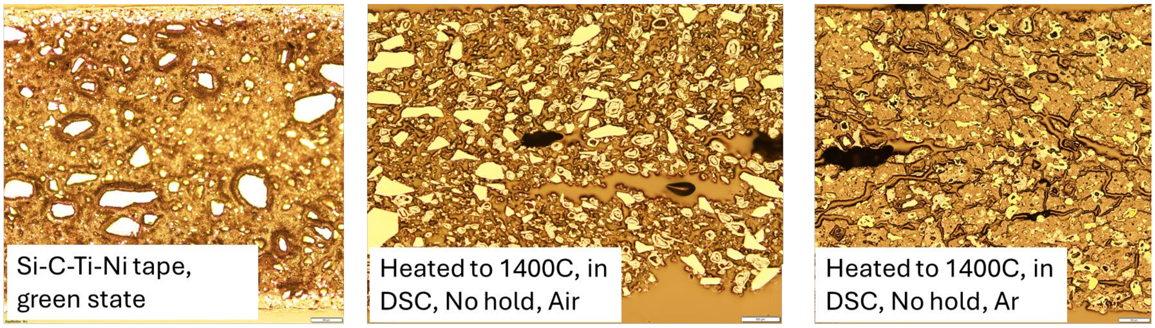

Si-C-Ti-Ni tape, green state

Heated to 1400C, in DSC, No hold, Air

Heated to 1400C, in DSC, No hold, Ar

Fig. 10 Optical micrographs capture microstructural changes when tape cast Si-C-Ti-Ni stack is heated in air vs. Ar, indicating reaction sintering happening under Ar.

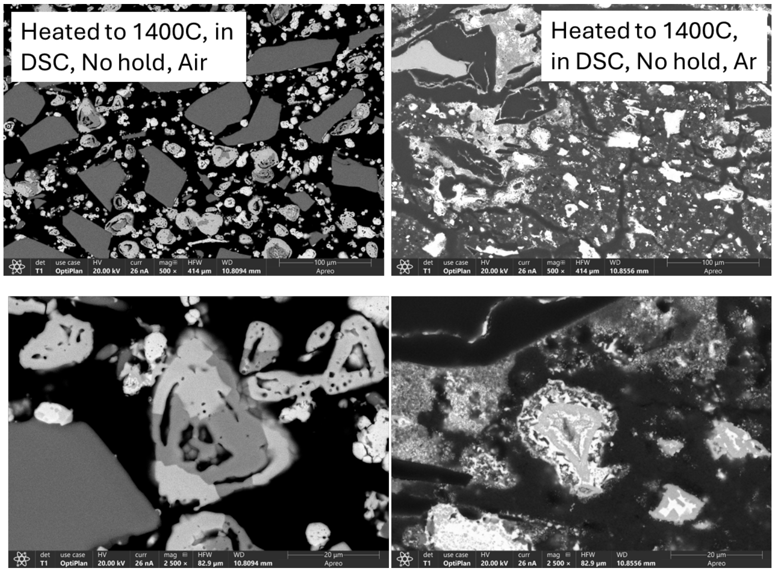

Fig. 11 SEM images obtained from heat treated composite Si-C-Ti-Ni stack. Extremely fine microstructure is noted when heat treatment is done under Ar.

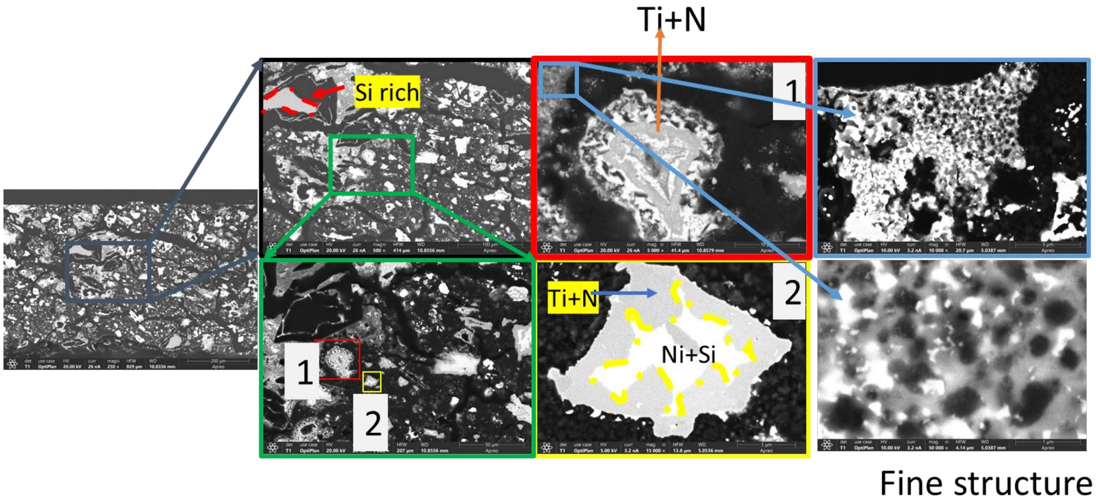

Fig. 12 Higher magnification SEM images of Ar- heat treated composite Si-C-Ti-Ni stack, showing chemical reaction between Ni and Si, and Ti and nitrogen. Also, formation of fine structure noted in Ni-Si reaction zone

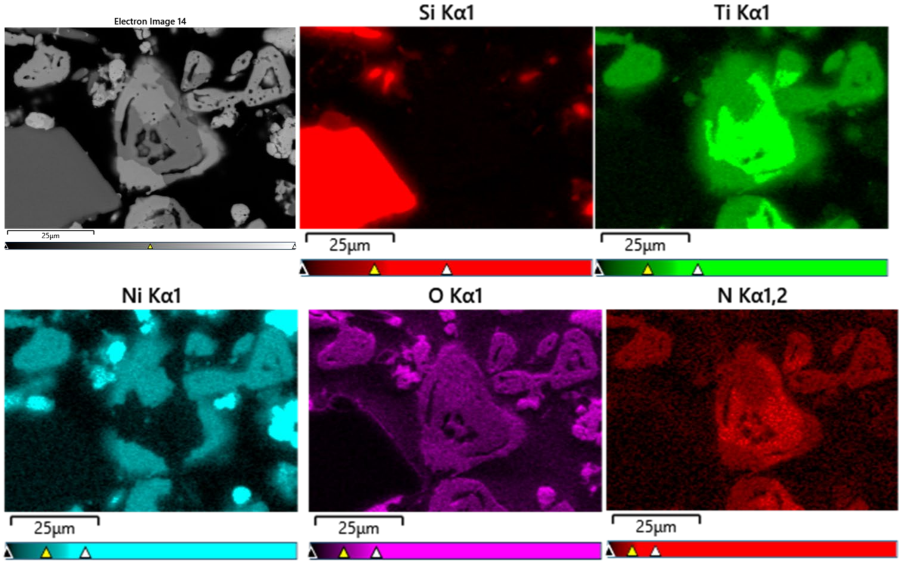

Fig. 13 EDS elemental map obtained from Si-C-Ti-Ni composite sample after air heat treatment at 1400C. Chemical reaction between Si, Ni and Ti is completely absent.

Reaction Sintering in Argon Atmosphere: Multi-Chemistry Tape-Cast Stacks

The differences in microstructure resulting from high-temperature sintering in air and argon environments prompted the decision to conduct reaction sintering trials exclusively under an argon atmosphere. After observing reaction sintering in single-layer composite Si-C-Ti-Ni tape-cast samples, further investigation focused on the behavior of multi-chemistry tape-cast laminated stacks during heat treatment.

A multi-layer stack consisting of Si-C, Ti, and Ni was assembled and subjected to heat treatment in an argon environment using a differential scanning calorimetry (DSC) instrument. The resulting microstructural changes were analyzed using scanning electron microscopy (SEM) and energy-dispersive X-ray spectroscopy (EDS), as presented in Figure 14. The SEM and EDS images clearly demonstrate that individual elemental powders within the multi-chemistry stack undergo chemical reactions during heat treatment in argon. According to EDS analysis, titanium and carbon react to form a titanium carbide (TiC) phase, while nickel and silicon combine to produce a nickel silicide phase. These chemical transformations confirm the effectiveness of the reactive sintering approach in argon for multi-chemistry laminated stacks.

The findings highlight the potential of employing multi-chemistry interlayer stacks for joining silicon carbide (SiC) substrates to structural alloys, such as 316L stainless steel. The ability to engineer targeted chemical reactions within laminated tape-cast stacks expands the possibilities for designing graded interlayers and optimizing ceramic-to-metal joints through controlled heat treatment in inert environments.

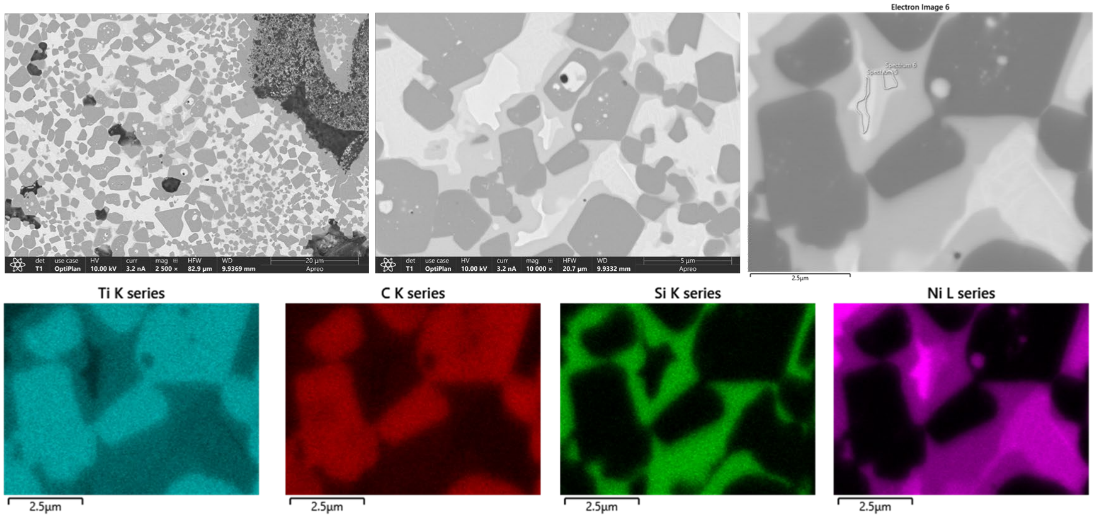

Fig. 14 Evidence of solid-state reaction between individual elements present in the multi-chemistry Si-C/Ti/Ni stack prepared by tape casting and subsequent lamination. Reaction between Ti and C, and Ni and Si is confirmed from EDS elemental maps.

Building on the successful demonstration of reaction sintering in multi-layer Si-C, Ti, and Ni stacks under an argon atmosphere, where targeted chemical interactions between elemental powders such as the formation of titanium carbide and nickel silicide were achieved, the approach was further expanded to explore additional reactive combinations. **Interlayer chemistry was systematically designed to identify additional elements capable of reaction sintering both with each other and the SiC matrix** . Powders of Ti, Ni, Mo, Cr, and W were combined in various proportions (by both equal weight percentage and equal volume percentage), then blended with SiC powders and formed into small pellets. These pellets underwent heat treatment trials in a differential scanning calorimeter (DSC), after which the SiC interface was thoroughly characterized.

Figure 15 displays SEM images depicting the interface between silicon carbide (SiC) and a mixed powder blend comprising titanium, chromium, nickel, molybdenum, and tungsten after heat treatment within a differential scanning calorimeter (DSC). The SEM imaging indicates notable microstructural transformations at the SiC interface, evidenced by changes in the morphology of the original elemental powder mixture. These findings suggest that active chemical interactions occur at the interface during the heat treatment process.

To provide further insight into the chemical composition at the SiC interface, EDS elemental mapping was conducted, as illustrated in Figure 16. The EDS results demonstrate a pronounced enrichment of chromium (Cr) at the SiC interface. Furthermore, chromium is closely associated with titanium (Ti) and molybdenum (Mo), forming a distinct phase, while a nickel-rich layer is situated between the silicon carbide region and the chromium-enriched area.

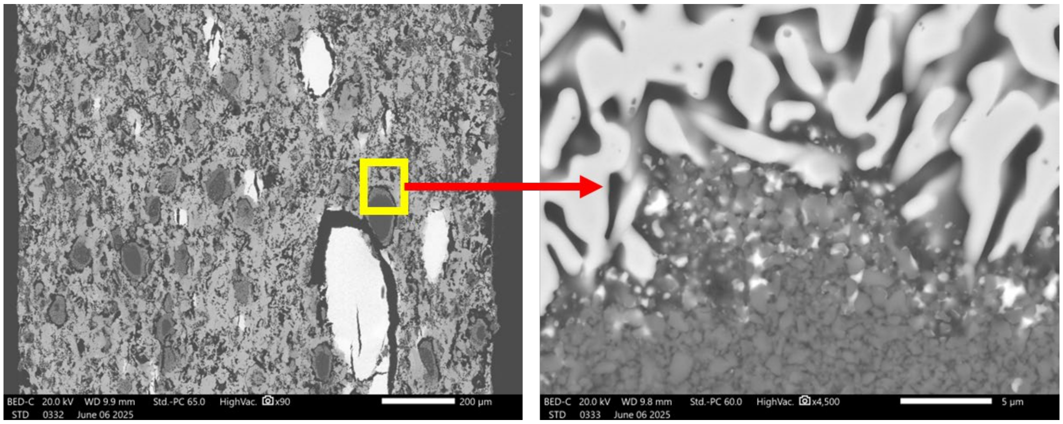

Fig. 15 SEM image of SiC-(Ti-Cr-Ni-Mo-W) interface after heat treatment under Ar inside DSC. Chemical reaction at SiC interface is evident.

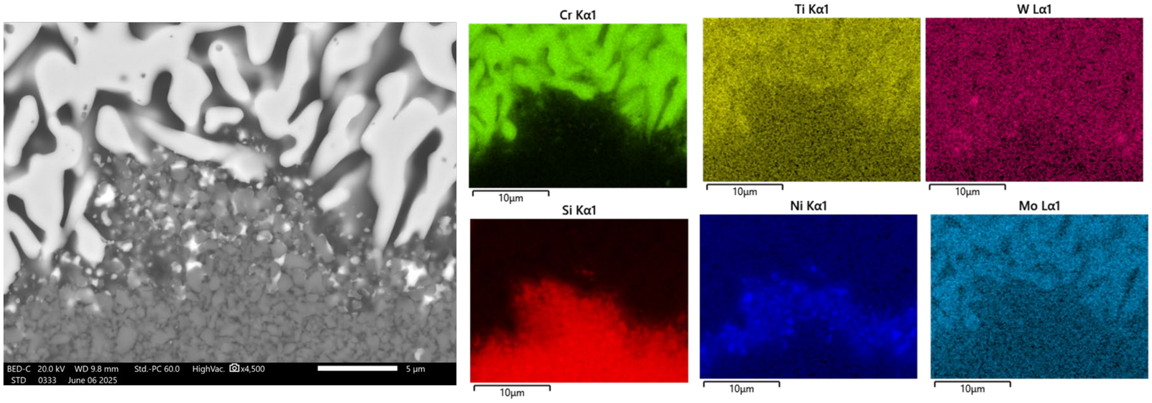

Fig. 16 EDS elemental map of SiC-(Ti-Cr-Ni-Mo-W) interface after heat treatment under Ar inside DSC.

Detailed characterization trials were performed on the SiC-(Ti-Cr-Mo-W) powder blend following heat treatment within DSC. The resulting microstructural images and corresponding EDS elemental mappings for this composition are presented in Figure 17. The analysis reveals clear evidence of chemical reactions occurring at the SiC interface, as indicated by significant morphological changes and distinct elemental distribution patterns captured in the EDS maps. The EDS mapping data suggest that, in the absence of Ni within the powder mixture, Si and W exhibit a strong association, remaining closely coupled at the interface. Cr is observed to localize between the silicon-rich SiC phase, acting as an interlayer. Meanwhile, Mo and Ti tend to react with each other, forming distinct phases. Additionally, there appears to be a compositional gradient of Mo present throughout the mixture.

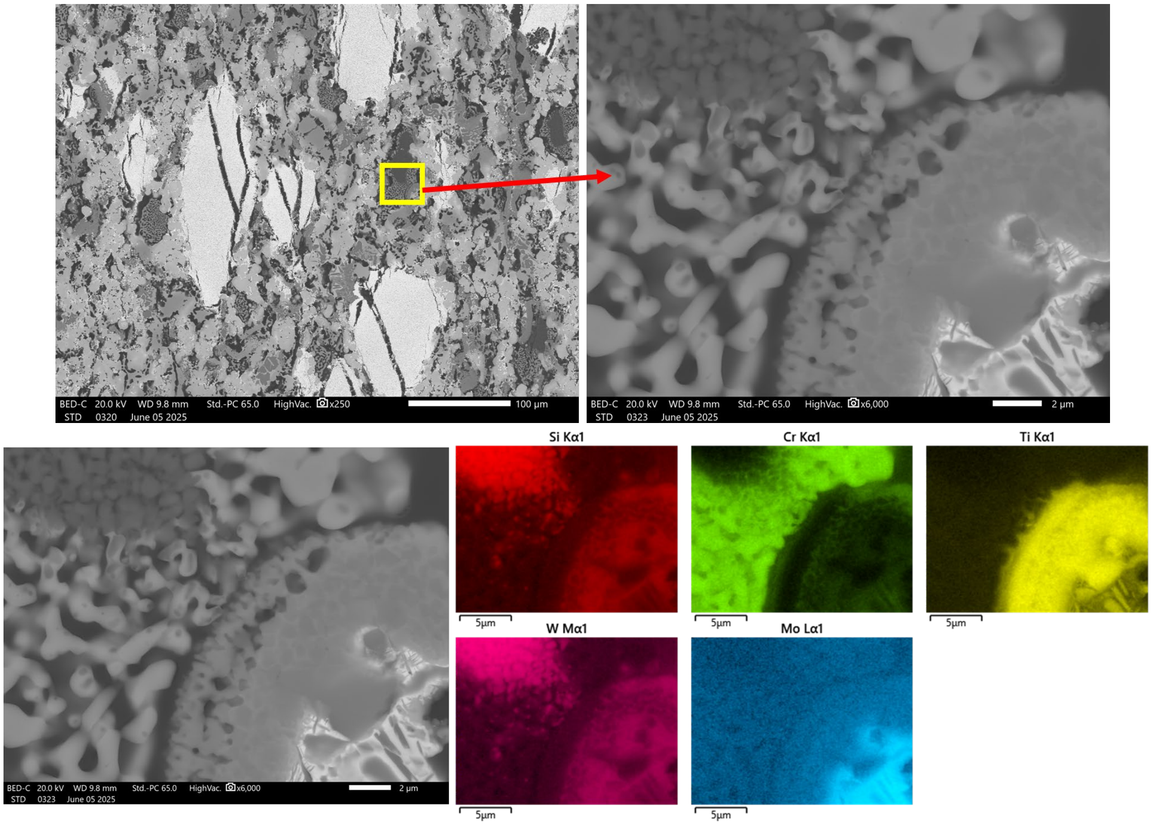

Fig. 17 SEM images and corresponding EDS elemental map of SiC-(Ti-Cr-Mo-W) powder mixture. Extensive reaction sintering is taking place at SiC interface.

Collectively, these observations confirm that the chosen combination of elemental powders effectively promotes reaction sintering at the SiC interface. The resultant microstructural and chemical modifications illustrate the potential of this powder blend to enable reliable joining between silicon carbide and metallic substrates, highlighting its promise for ceramic-to-metal joining applications.

4.0 Bulk Specimen Joining to Show SiC-Metal Reaction Bonding via Graded Tape-Cast Interlayer

Based on DSC analysis of small-scale heat treatment studies, potential tape cast interlayer candidates were identified for use in bulk-scale joining experiments between bulk SiC substrate and bulk 316L SS blanks. Following interlayers have been studied:

(i) multi-stack (Si+C/Ti/Ni) interlayer,
(ii) multi stack (316LSS/Mix-1) interlayer – [Mix-1 = Ti-Cr-Ni-Mo-W]
(iii) multi stack (316LSS/Mix-2) interlayer – [Mix -2 = Ti-Cr-Mo-W]

Figure 18 shows the joint coupon assembly, dimensions and the furnace that has been used for the joining trial studies.

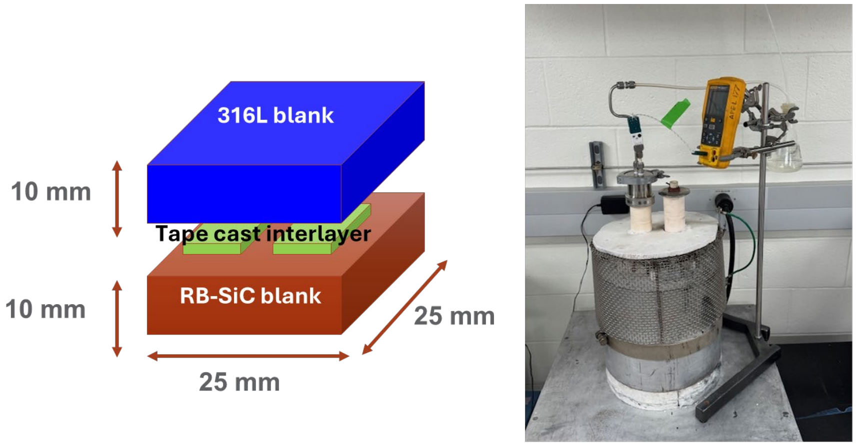

Fig. 18. RB-SiC to 316LSS blank joining at bulk scale using tape cast interlayer. A vertical tube furnace with protective Ar environment has been used for bulk scale heat treatment

Joining trial using Si+C/Ti/Ni tape cast interlayer

In the preliminary joining experiment, a stack consisting of Si-C/Ti/Ni was layered onto an RB-SiC substrate. The assembly underwent heat treatment in an argon atmosphere at 1400C. Analysis of the resulting microstructure, particularly the micrograph presented in Fig. 19a, reveals that a close metallurgical bond was established between the tape cast stack and the RB-SiC substrate. However, the tape cast layer exhibited several large voids. These voids are attributed to the high organic binder content used during slurry preparation; during the high-temperature heat treatment, the binder burned out, resulting in significant porosity. To address this issue and enhance densification, subsequent slurry preparations utilized a much lower binder content.

SEM images of the bond interface demonstrated the formation of a highly adherent coating on the RB-SiC, extending several millimeters along the interface. EDS elemental mapping, as shown in Fig. 19 (b), (c), and Fig. 20, confirmed the presence of SiC whiskers and a Si-rich phase at the bond interface. These features suggest a potential mechanism for the bonding process. Additionally, traces of nickel (Ni) were identified in both the tape cast interlayer and within the RB-SiC substrate itself. This observation indicates that Ni diffused into Si-rich regions, consistent with the strong chemical affinity between Ni and Si.

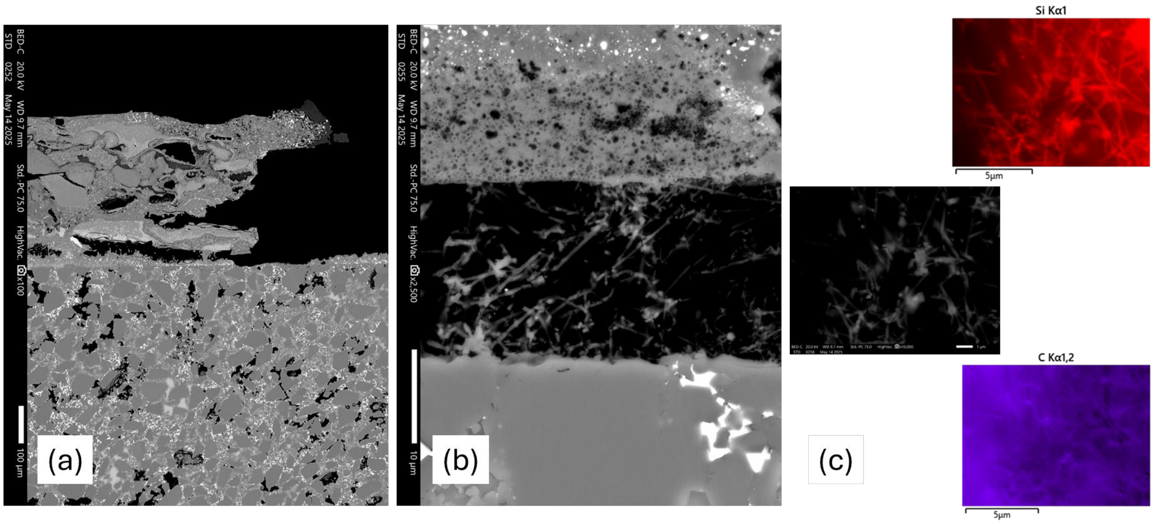

Fig. 19 Intimate metallurgical bonding is noted at the interface between RB-SiC and tape cast (Si+C/Ti/Ni) interlayer. (a) SEM image of joint interface (b) joint interface at a higher magnification showing bonding mechanism, and (c) EDS map of the joint interface shows formation of SiC whiskers, acting as bridges for joining with the RB-SiC substrate.

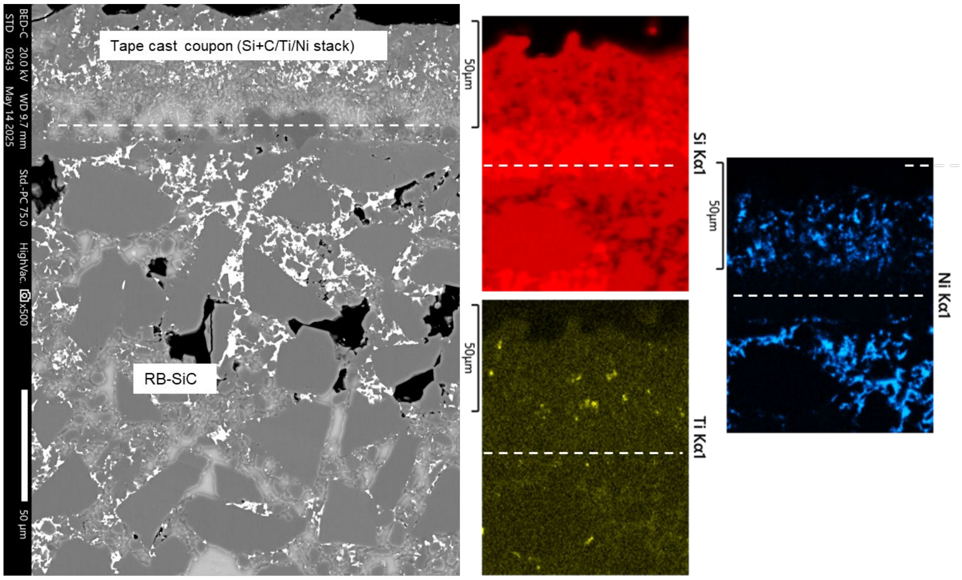

Fig. 20 EDS elemental map data from RB-SiC and tape cast multi-chemistry stack (Si+C/Ti/Ni) after high temperature heat treatment in Ar. Si-rich phase formation along with diffusion of Ni is noted.

<u>Joining trial using</u> **<u>multi stack (316LSS/Mix-1) interlayer</u> – Mix 1 (Ti-Cr-Ni-Mo-W)**

For the second joining trial, an interlayer composed of 316L stainless steel and Mix-1 (Ti-Cr-Ni-Mo-W) was utilized. Tape-cast interlayer sections, each cut into 5 mm squares, were positioned between the RB-SiC substrate and a blank of 316L stainless steel. The assembled stack then underwent heat treatment in an argon atmosphere at two distinct temperatures.

After completion of the heat treatment process at 1390C, the joint was cross-sectioned to allow for thorough characterization of the interface. Analytical techniques employed included optical microscopy (OM), SEM, and EDS elemental mapping. These methods were used to examine the microstructural features and chemical composition at the bond interface. Fig. 21 shows a low-magnification OM of the joint cross section. A thick interaction layer is visible at the joint interface between 316L SS blank and RB-SiC substrate, indicating very good metallurgical bonding. Fig. 22 and Fig. 23 provide additional information about the interaction layer, confirming intimate metallurgical bonding between RB-SiC and 316L SS blank, when Mix-1 (Ti-Cr-Ni-Mo-W) is used as interlayer. Fig. 24 shows SEM image of joint cross section, when heat treatment was carried out at 1375C. Confirmation of strong metallurgical bonding is confirmed.

Vickers microhardness testing was conducted to assess the mechanical strength of the Mix-1 interlayer region, RB-SiC matrix, and 316L SS blank (see Fig. 24). The RB-SiC matrix exhibited high hardness (~2400 VHN), as anticipated. The interlayer region demonstrated moderate hardness (~1200 VHN), while the 316L SS sample displayed significantly lower hardness (130 VHN). These results indicate that the chosen tape-cast interlayer composition possesses satisfactory mechanical strength. However, additional shear testing is recommended to obtain further insights.

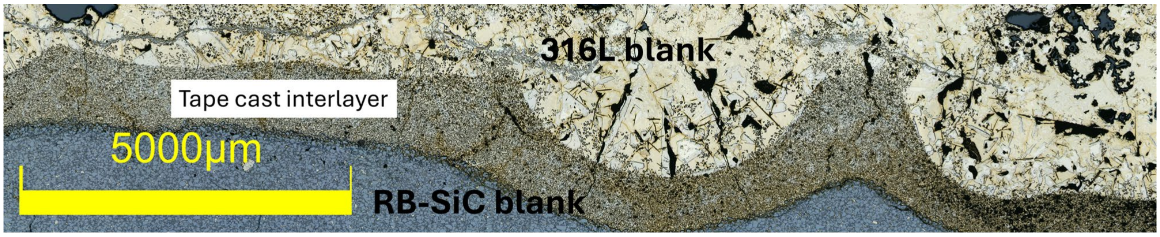

Fig. 21 Low-magnification OM of RB-SiC to 316L SS blank joint using Mix-1 (Ti-Cr-Ni-Mo-W) interlayer. A thick interaction layer is visible at the joint interface. T = 1390C

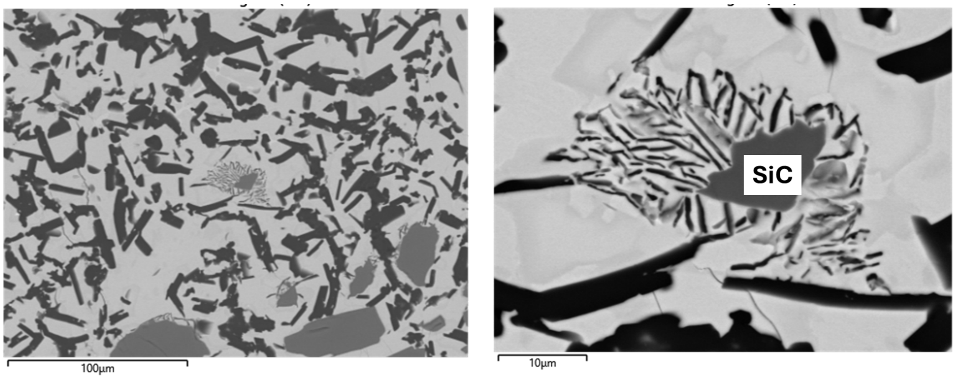

Fig. 22 SEM images from the interaction layer show clear evidence of SiC particles reacting with Mix-1 tape cast interlayer.

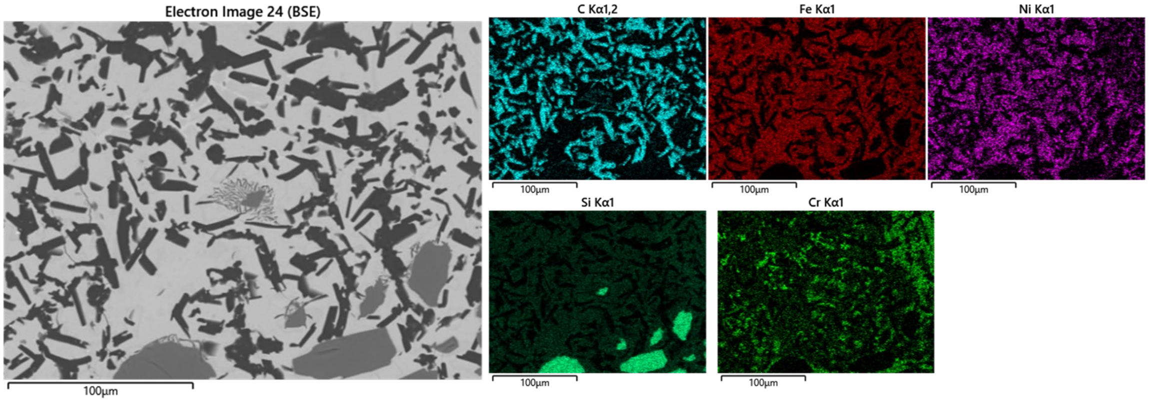

Fig. 23 EDS elemental mapping of the interaction layer. Strong chemical reaction is noted between SiC and Ti-Cr-Ni-Mo-W tape cast interlayer. Precipitation of carbon in the form of graphite flakes, alloying between Fe and Ni is notable in the reaction zone.

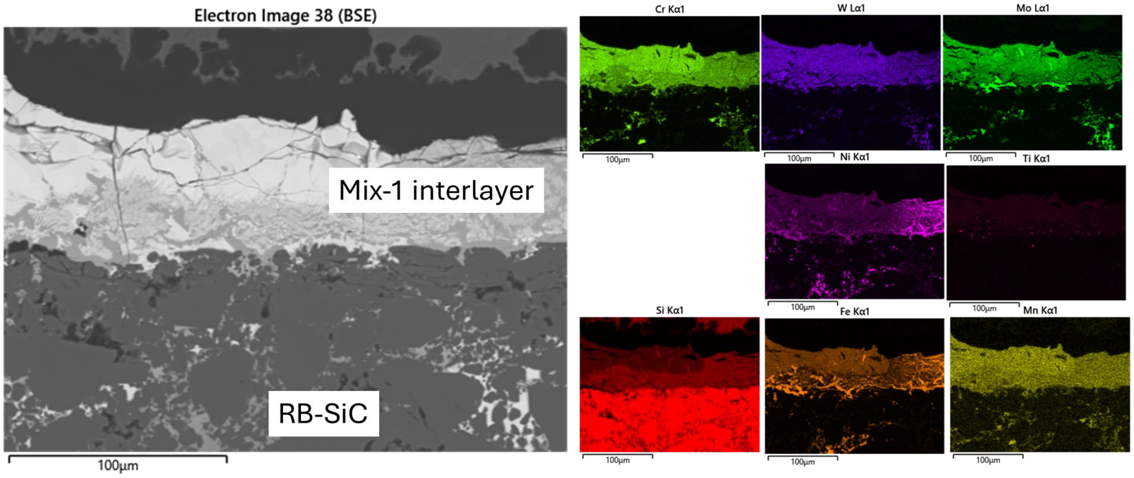

Fig. 24 RB-SiC and 316L SS blank joined using Mix-1 interlayer at T= 1375C. EDS elemental mapping of the interaction layer confirms metallurgical bonding, through alloying between various elements between themselves and with Si.

In conclusion, Mix-1 chemistry demonstrates significant potential for establishing robust metallurgical bonds with RB-SiC. The elemental metal powder mixture can chemically interact with RB-SiC while preserving its metallic properties and avoiding the formation of multiple compounds.

Joining trial using multi stack (316LSS/Mix-2) interlayer **– Mix 2 (Ti-Cr-Mo-W)**

In the third joining trial, an interlayer consisting of 316L stainless steel and Mix-2, was used. The tape-cast interlayer was positioned between the RB-SiC substrate and a blank of 316L stainless steel, as illustrated in Fig. 18. The assembled joint underwent heat treatment at a temperature of 1375°C.

SEM images of the joint cross-section, along with EDS elemental maps, are presented in Fig. 25. The use of the Mix-2 interlayer resulted in effective bonding on the 316L stainless steel blank side, as indicated in Fig. 25. The detection of Si at the joint interface near the 316L stainless steel blank confirms substantial interdiffusion of elements during the joining process. Analysis suggests that silicon (Si), tungsten (W), and molybdenum (Mo) form an alloy within the joint interlayer after the heat treatment. In contrast, chromium (Cr), titanium (Ti), and manganese (Mn) tend to alloy near the interface with the 316L stainless steel blank. These observations indicate robust intermixing among the elemental powders that constituted the tape-cast interlayer.

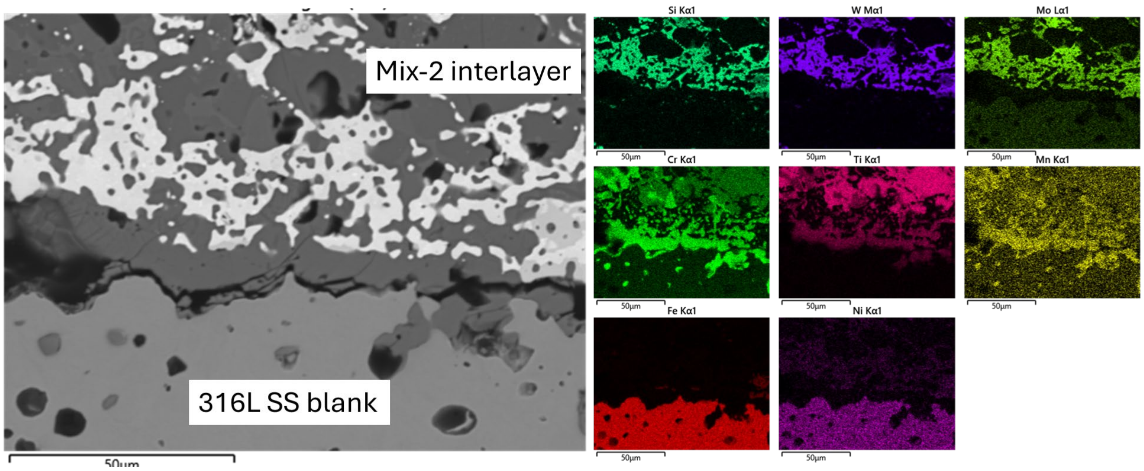

Fig. 25 RB-SiC and 316L SS blank joined using Mix-2 interlayer at T= 1375C. EDS elemental mapping of the interaction layer confirms metallurgical bonding with 316L SS, but not with RB-SiC.

Overall, the elemental powder blend used to fabricate the Mix-2 tape-cast interlayer demonstrates promising compatibility for joining applications with 316L stainless steel blanks, as evidenced by the good metallurgical bonding and significant elemental intermixing at the joint interface.

Final joining assembly trial using multi stack (316LSS/Mix-2/Mix-1) interlayer

Building upon the outcomes of previous bulk scale joining trials, a final trial was conducted utilizing a multi-stack tape cast interlayer composed of three distinct layers. The design of this assembly was informed by prior observations: Mix-1 (CrTiNiMoW) exhibited strong bonding with RB-SiC, while Mix-2 (CrTiMoW) demonstrated effective bonding with 316L stainless steel (SS). Tape casting slurry was prepared with less than 1 wt.% binder to maximize densification after sintering.

The multi-stack tape cast interlayer was structured as follows:

- ***First layer: Mix-1 (CrTiNiMoW)***
- ***Second layer: Mix-2 (CrTiMoW)***
- ***Third layer: 316L SS***

For the joining trial, the interlayer assembly was positioned on the RB-SiC substrate with the Mix-1 layer placed directly adjacent to the RB-SiC side. This arrangement was selected to optimize bonding across both interfaces, leveraging the compatibility of each mix with its respective substrate. **The complete assembly underwent heat treatment at 1400°C in an argon (Ar) atmosphere.** This thermal process was intended to promote interlayer bonding and metallurgical interactions between the stacked layers and the substrate materials.

Figure 26 provides an overview of the joint following heat treatment, accompanied by a low-magnification cross-sectional image. The image distinctly reveals strong metallurgical bonding at the interface between RB-SiC and the adjacent material, for several mm length. Additionally, a densified interlayer is observed, indicating that the tape cast chemistry recipe has been successful in facilitating metallurgical bonding between RB-SiC and metallic components.

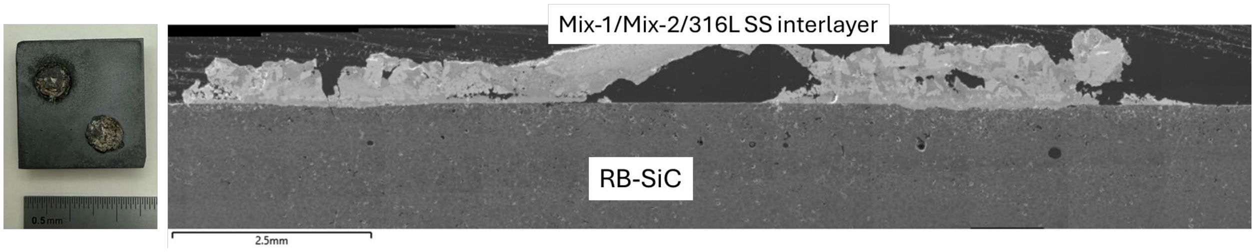

Fig. 26 RB-SiC to tape cast interlayer joint top view and cross section image. Heat treatment T = 1400C. Tape cast interlayer is made of Mix-1, Mix-2 and 316L SS. Mix-1 side was placed adjacent to RB-SiC. *Very strong metallurgical bonding between RB-SiC and tape cast interlayer is observed*.

Figure 27 presents a higher magnification SEM image of the joint assembly, accompanied by EDS elemental map data. The EDS mapping distinctly demonstrates significant elemental intermixing and interdiffusion among the various elements present in the joint. This observation confirms the effectiveness of the tape cast composition and the specific configuration employed in the assembly process to join RB-SiC to 316L SS.

The analysis reveals that W and Mo exhibit a strong affinity for Si, resulting in the formation of distinct phases. Additionally, Cr, Fe, Ni, and Ti are observed to have mutual affinity, leading to the formation of various phases with different morphologies within the joint structure.

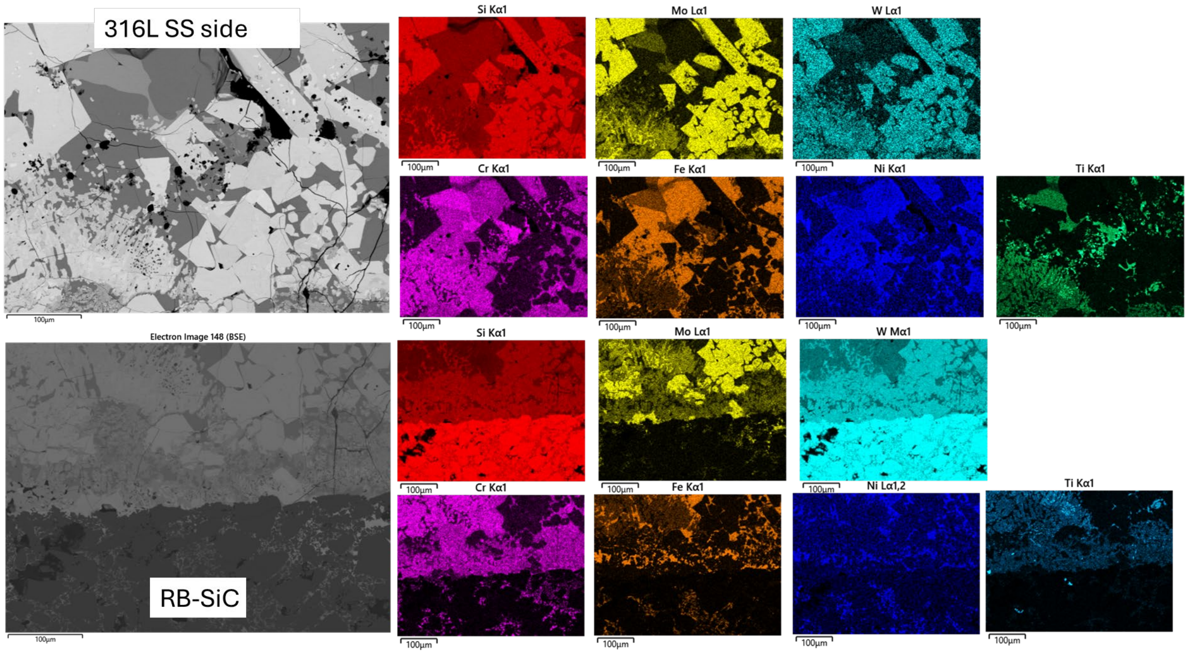

Fig. 27 RB-SiC to tape cast interlayer joint cross section image, and EDS map data. Significant interdiffusion, and strong metallurgical bonding with RB-SiC is confirmed. Heat treatment T = 1400C.

5.0 Conclusions and Outlook:

The tape casting process has been utilized in this research as an innovative approach to achieve metallurgical bonding between silicon carbide (SiC) and structural metals such as 316L stainless steel. Silicon carbide, a non-oxide ceramic, is known for its outstanding mechanical properties, resistance to chemical corrosion, high thermal stability, and suitability for demanding high-temperature applications. Despite its desirable properties, joining silicon carbide to structural metals poses significant challenges due to its covalent bonding nature. Traditional joining methods often fail to create a robust interface between SiC and metals like 316L stainless steel.

This study explored the use of solid-state techniques, specifically powder metallurgy-based methods and layer-wise additive manufacturing concepts, to engineer a graded interface. This interface serves as an effective bridge between silicon carbide and structural metals, facilitating strong bonding.

The research demonstrates that tape casting is a versatile method for rapidly screening new compositions and fabricating multilayer structures with tailored properties. This technique can accelerate the development of compositionally graded or functionally graded interfaces. Several promising compositions have been identified that enable joining silicon carbide to structural metals. **In particular, the work has shown successful joining of reaction-bonded silicon carbide (RB-SiC) to 316L stainless steel through high-temperature sintering experiments, resulting in strong metallurgical bonding at the interface.**

Outlook:

The research conducted in this project has demonstrated a viable pathway for joining reaction-bonded silicon carbide (RB-SiC) to structural metals such as 316L stainless steel through the development of compositionally graded, tape-cast interlayers. Building upon these successes, several forward-looking opportunities emerge that can meaningfully advance the maturity, applicability, and deployment potential of this joining methodology. Following next steps are recommended.

1. Detailed Mechanical and Environmental Qualification

Preliminary microhardness measurements indicate promising bonding strength within interlayer regions; however, comprehensive mechanical evaluation is critical for deployment in CSP receivers and other high-temperature systems. Relevant mechanical testing such as lap-shear, 4-point bend etc., as recommended by ASTM, should be carried out to learn about SiC to metal joint strength. In addition, thermomechanical fatigue evaluations, creep assessments above 1000 °C, and detailed failure-mode analysis should be performed. Environmental testing under oxidizing and cycling conditions will further establish reliability for long-duration operation in solar thermal plants.

2. Heat Treatment Optimization

RB-SiC to 316L SS joining has been achieved by carrying out sintering experiments at ~1400C in Ar environment. Further optimization is needed to improve bonding between the tape cast interlayer alloy and the RB-SiC substrate. Factors to consider include furnace environment (vacuum or inert gas), heat treatment duration, and alternative heating methods such as Joule heating. These steps are essential for optimizing the two-step heat treatment process for joining with the metal substrate, e.g. 316L SS or similar.

3. Optimizing Tape Casting and Interlayer Chemistry to Enable Joining Additional Structural Alloys with SiC.

The multi-chemistry tape-casting method has demonstrated that carefully designed gradients in composition and phase formation can successfully address mismatches between ceramic and metal properties. Future studies should aim to further improve interlayer chemistries by testing other refractory elements, fine-tuning layer thicknesses, and adjusting powder properties. This research confirmed that 316L stainless steel can be joined by modifying tape-cast layer chemistries, and a similar strategy could be applied to join silicon carbide with other structural metals, such as nickel-based alloys.

4. Scaling Toward Component-Level Demonstrations

With successful bulk-scale joining trials using Mix-1, Mix-2, and hybrid configurations, the next technical milestone is application-scale demonstration. Fabricating and testing SiC absorber segments joined to shaped metallic housings will enable validation of manufacturability, sealing strategies, pressure containment, and long-term structural stability. Such component-level studies will accelerate readiness for CSP receiver integration. Active collaboration with relevant industry partners is recommended for component-level demonstrations.

5. Broader Application Across Advanced Energy Systems and Scope of Additive Manufacturing and Digital Design

The reaction-sintering-assisted graded interface technique enables joining SiC to various alloys, including Ni-based superalloys and ferritic steels, supporting DOE applications such as heat exchangers, hydrogen production, fusion energy, and industrial decarbonization. Customizing interlayer chemistries can broaden this method's impact. With tape-casting and powder-metallurgy compatible with layered deposition, future research may incorporate digital design and additive manufacturing for precision interlayers, rapid screening, and seamless integration in complex metallic components.

Reference(s)

1. Volumetric receivers in Solar Thermal Power Plants with Central Receiver System technology: A review https://doi.org/10.1016/j.solener.2011.02.002

2. High-temperature, point-focus, pressurised gas-phase solar receivers: A comprehensive review https://doi.org/10.1016/j.enconman.2019.02.020

3. High-Performance SiC–Based Solar Receivers for CSP: Component Manufacturing and Joining https://doi.org/10.3390/ma14164687

4. Two novel high-porosity materials as volumetric receivers for concentrated solar radiation. https://doi.org/10.1016/j.solmat.2004.02.009

5. Brazing of Silicon Carbide to Stainless Steel. Am. Ceroni. Soc. Bull., 64 [2] 322-24 (1985)

Pacific Northwest National Laboratory

902 Battelle Boulevard
P.O. Box 999
Richland, WA 99354

1-888-375-PNNL (7665)

www.pnnl.gov